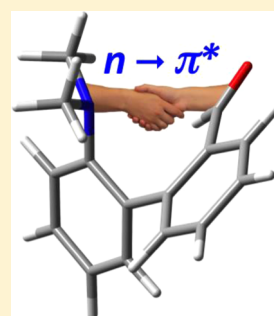


# Substituted 2-(Dimethylamino)biphenyl-2'-carboxaldehydes as Substrates for Studying $n \rightarrow \pi^*$ Interactions and as a Promising Framework for Tracing the Bürgi–Dunitz Trajectory

Gary W. Breton<sup>\*,†</sup> and Chiquito J. Crasto<sup>‡</sup><sup>†</sup>Department of Chemistry, Berry College, Mount Berry, Georgia 30149, United States<sup>‡</sup>Center for Biotechnology and Genomics, Texas Tech University, Lubbock, Texas 79409, United States

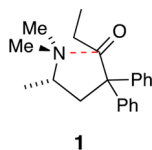
## S Supporting Information

**ABSTRACT:** The Bürgi–Dunitz trajectory traces points along the pathway of bond formation between a nucleophile and electrophile. Previous X-ray crystallographic studies of some molecules containing a nucleophilic nitrogen atom and electrophilic carbonyl group provided some initial evidence for various degrees of bond formation via initial  $n \rightarrow \pi^*$  interactions. Observation of a complete set of points along the trajectory, however, has not yet been attained. In this paper, we present a DFT computational study investigating substituted 2-(dimethylamino)biphenyl-2'-carboxaldehydes as substrates for further examination of  $n \rightarrow \pi^*$  interactions and as a potential framework for more complete tracing of the Bürgi–Dunitz trajectory. These compounds are particularly suitable for study because of the rotational freedom granted by the C–C bond connecting the two aromatic rings allowing the molecule to choose the degree of interaction between the two complementary groups. The extent of interaction is measured by interatomic distance, NBO second-order perturbative analysis energies, volume of transferred electron density as provided by ETS–NOCV analysis, and differences in energies between models that allow for  $n \rightarrow \pi^*$  interactions and those that do not. A series of substituted biphenyls are ultimately identified as future synthetic targets that have maximum potential for providing improved tracing of the Bürgi–Dunitz trajectory.



## INTRODUCTION

Evidence for intramolecular donor–acceptor interactions between the lone pairs of suitably positioned heteroatoms and accessible carbonyl group carbons (i.e.,  $n \rightarrow \pi^*$  electron donation) was cleverly provided by Bürgi et al. in 1973 via an analysis of the X-ray crystal structures of a series of compounds, including (S)-methadone **1** (below), that could adopt conformations that allowed a nucleophilic nitrogen atom in the molecule to move into the proximity of an electrophilic carbonyl group.<sup>1</sup> The observed N–C interatomic distance for **1** of 2.91 Å was found to be less than the sum of the van der Waals radii of C and N (3.25 Å), indicative of an apparently stabilizing  $n \rightarrow \pi^*$  electronic interaction (illustrated by a dashed red line in **1**).



Further studies conducted on a variety of molecular frameworks have demonstrated that these stabilizing interactions are not uncommon.<sup>2,3</sup> Allinger estimated the stabilizing energy of  $n(\text{N}) \rightarrow \pi^*(\text{C}=\text{O})$  interactions to be on the order of 1–2 kcal/mol on the basis of model systems.<sup>3</sup> Recently, there have been several studies that describe the roles that similar interactions between oxygen atom lone pairs and amide

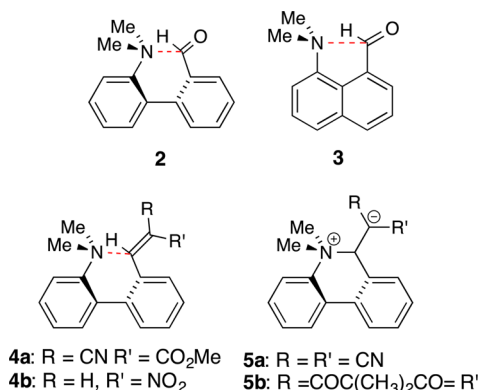
carbonyl groups play in the structural stabilities of proteins.<sup>4</sup> Again, while the magnitude of the individual interactions has been estimated to be on the order of only 1–2 kcal/mol, the additive effects, like the cumulative effect of multiple hydrogen bonds, could be quite significant.<sup>4b</sup>

Wallis studied model system **2** in which the dimethylamino group on one ring of a biphenyl system is capable of interacting with an aldehyde group on the neighboring benzene ring.<sup>2d,f</sup> Unlike the more extensively studied 1,8-disubstituted naphthalene compounds **3**,<sup>2e,g,5</sup> in which there is essentially “forced” interaction between the *peri*-substituted groups because of inescapable proximity, the biphenyl framework allows the molecule to “choose” the extent of interaction between the nitrogen atom and the carbonyl group by rotation about the central C–C  $\sigma$  bond. If the interaction is favorable, the two groups should be drawn together, resulting in a shorter distance between the nitrogen and carbon atoms and a diminished dihedral angle between the two benzene rings. The X-ray crystal structure of **2** revealed an N–C interatomic distance of 2.989 Å which, again, is less than the sum of the van der Waals radii of the two atoms.<sup>2d,f</sup> The nitrogen atom is opportunistically turned such that its lone pair is directed toward the  $\pi^*$  orbital of the carbonyl carbon atom ( $\angle \text{NCO} = 126.5^\circ$ ) allowing for transfer of some of its electron density into the electrophilic

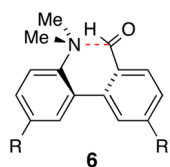
Received: April 7, 2015

Published: July 8, 2015

$\pi^*$  orbital. These observations, like those of **1**, are consistent with a stabilizing electronic interaction between the two groups. Wallis attempted to alter the nature of the electrophilic carbon atom using variously substituted vinyl substituents in place of the carbonyl group (compounds **4** and **5**) in an apparent effort to find points along what is referred to as the Bürgi–Dunitz trajectory, i.e., the trajectory tracing increasing degrees of N–C bond formation.<sup>1,2d</sup> However, the molecules Wallis chose to include in the study could ultimately only be loosely grouped into two categories: those in which a simple “intermolecular-like”  $n \rightarrow \pi^*$  interaction between the two groups was observed (**4a,b**) and those in which a fully formed N–C  $\sigma$  bond was observed (**5a,b**).



We wondered whether the extent of interaction between the two groups might be more delicately controlled by varying the nature of substituents on the aromatic rings of the biphenyl system (i.e., R and R' in **6**). Electron-withdrawing groups situated *para* to the aldehyde group (i.e., R' in **6**) were predicted to increase the electrophilicity of the carbonyl group and thereby solicit increased delocalization of the nitrogen lone pair electrons into the  $\pi^*$  orbital, while electron-donating groups in the same position should attenuate the interaction. On the contrary, electron-donor groups substituted *para* to the dimethylamino group (i.e., R in **6**) should have the effect of increasing electron density at the nitrogen lone pair, which should facilitate charge transfer into the carbonyl  $\pi^*$  orbital, while electron-withdrawing groups at the same position should have the opposite effect. We hoped that by investigating a series of suitably substituted biphenyl systems that we might be able to clearly trace the Bürgi–Dunitz trajectory. To this end, we employed DFT theory to analyze the effects that varying substituents on the aromatic rings have on the  $n \rightarrow \pi^*$  interactions. We further explored the nature and energetics of the interactions via ETS–NOCV and NBO analyses.



## RESULTS AND DISCUSSION

**1. Computational Studies of 2-(Dimethylamino)-biphenyl-2'-carboxaldehyde (**2**).** Our initial efforts were focused on locating a convenient computational protocol that would allow for the study of 2-(dimethylamino)biphenyl-2'-carboxaldehyde (**2**) and appropriately substituted derivatives

(**6**) with both acceptable accuracy and reasonable computational resources. All geometry optimizations were carried out using the Gaussian 09 suite of programs.<sup>6</sup> We began by applying density functional theory toward optimizing the structure of **2** and comparing the result to experimental values as provided by the reported X-ray crystal structure.<sup>2d,f</sup> DFT optimization of **2** using the B3LYP functional (which had already been demonstrated to be a good choice for modeling biphenyl compounds and for NBO analyses of similar  $n \rightarrow \pi^*$  interactions),<sup>7</sup> and the robust 6-31G(d) basis set afforded reasonable agreement with key structural data obtained via X-ray crystallography (entries 1 and 2 in Table 1 and Figure 1).<sup>2d</sup>

**Table 1.** Effect of Basis Set and solvent on the DFT-Minimized Structure of **2** and Comparison to Experimental Data<sup>a</sup>

entry	basis set	solvent	$d_1$ (Å)	$d_2$ (Å)	$\alpha$ (deg)	$\Theta^c$ (deg)
1	experimental X-ray data <sup>b</sup>		2.989	1.207	58.58	2.42
2	6-31G(d)		2.958	1.218	55.47	2.36
3	6-31+G(d)		2.946	1.221	55.32	2.36
4	6-31++G(d)		2.943	1.221	55.23	2.40
5	6-311G(d,p)		2.935	1.212	55.08	2.32
6	6-311+G(d,p)		2.964	1.214	55.95	2.22
7	6-311+G(2d,p)		2.984	1.212	56.75	2.03
8	6-31G(d)	CHCl <sub>3</sub>	2.940	1.222	55.99	2.49
9	6-31G(d)	CH <sub>3</sub> OH	2.931	1.223	54.79	2.53
10	6-31G(d)	DMSO	2.930	1.223	54.78	2.48
11	6-31G(d)	H <sub>2</sub> O	2.930	1.223	54.78	2.48

<sup>a</sup>The DFT B3LYP functional was used throughout. All structures were confirmed to be minima by frequency calculations. <sup>b</sup>Reference 2d. <sup>c</sup>The angle  $\Theta$  measures the deflection of the carbonyl oxygen bond from the plane defined by the carbonyl carbon and the hydrogen and carbon atoms to which it is attached, as illustrated in the graphic.

In particular, the calculated distance between the amino group nitrogen atom and the carbonyl carbon (2.958 Å) and the CO bond length (1.218 Å) agreed fairly well with the experimental values of 2.989 and 1.207 Å, respectively. As in the crystal structure, the nitrogen atom lone pair is favorably disposed toward interaction with the  $\pi^*$  orbital of the carbonyl group.

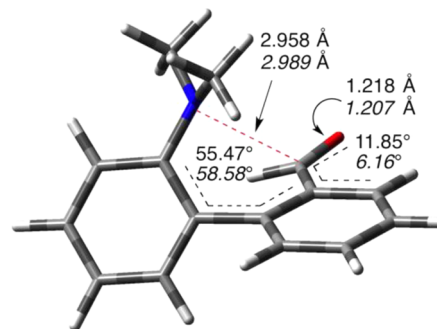


**Figure 1.** Optimized structure of biphenyl compound **2** at the B3LYP/6-31G(d) level with key structural measurements indicated (X-ray crystallographic data in italics).<sup>2d</sup>

The calculated  $\angle\text{NCO}$  value of  $122.2^\circ$  was in reasonable agreement with the experimental value of  $126.5^\circ$ . These angles are somewhat larger than the generally preferred angle for a nucleophilic attack on a carbonyl group ( $\sim 110^\circ$ ), but bond formation is still in its infancy (i.e.,  $\sim 3 \text{ \AA}$  away). Additionally, structural restrictions imposed by the biphenyl backbone of the system could also potentially prevent optimal orientation. In both the experimentally determined crystal structure and theoretically optimized structure, the carbonyl group was found to be rotated slightly out of the plane of the aromatic ring with a dihedral angle relative to the ring of  $6.16^\circ$  (experimental) and  $11.85^\circ$  (theoretical). The degree of pyramidalization of the carbonyl carbon resulting from the interaction was ascertained by calculating the angle of deflection ( $\Theta$ ) of the carbonyl oxygen atom from the plane defined by the carbonyl carbon and the hydrogen and aromatic carbon atoms to which it is attached, as has been done elsewhere (see graphic in Table 1).<sup>2a,b,4f</sup> Again, reasonable agreement between the experimental ( $2.42^\circ$ ) and theoretical ( $2.36^\circ$ )  $\Theta$ -values were obtained.

Structural changes resulting from minimizations employing increasingly complex basis sets via introduction of diffuse and/or polarization functions demonstrated no obvious patterns (Table 1). Geometry optimization using the costly 6-311+G-(2d,p), however, afforded a N--C bond distance of  $2.984 \text{ \AA}$  that agreed best with the experimental value. Because of the relatively low sensitivity of the geometry to the nature of the basis set, in conjunction with the number and complexity of the structures we anticipated analyzing, we settled on optimizing all of the structures at the B3LYP/6-31G(d) level of theory while applying the more expensive B3LYP/6-311+G(2d,p) level of theory for single-point energy calculations.

Inclusion of implicit solvent effects by application of the polarizable continuum model (PCM) using the integral equation formalism variant (IEFPCM) yielded some interesting effects (Table 1).<sup>8</sup> Conducting the geometry optimization in chloroform ( $\epsilon = 4.7$ ) decreased the N--C interatomic distance from  $2.958 \text{ \AA}$  in the gas phase to  $2.940 \text{ \AA}$  in solution. The C=O bond length slightly increased in response from  $1.218 \text{ \AA}$  (gas phase) to  $1.222 \text{ \AA}$  (solution). Greater pyramidalization of the carbonyl group ( $\Theta = 2.49^\circ$ ) was also observed. These changes are consistent with a greater extent of charge transfer from the nitrogen lone pair into the carbonyl  $\pi^*$  orbital due to the ability of the solvent to stabilize increased partial charge build up on the nitrogen and carbonyl oxygen atoms. The  $\angle\text{NCO}$  angle tightened up slightly from  $122.2^\circ$  in the gas phase to  $121.7^\circ$  in solution. Conducting the minimizations in more polar solvents such as methanol ( $\epsilon = 32.6$ ), DMSO ( $\epsilon = 46.8$ ), or water ( $\epsilon = 78.4$ ) all had the common effect of further shortening the N--C distance (to  $2.930 \text{ \AA}$ ), slightly increasing the C=O bond length (to  $1.223 \text{ \AA}$ ), tightening of the dihedral angle  $\alpha$ , but having little effect on the extent of pyramidalization of the carbonyl carbon (i.e.,  $\Theta$ ).

We were able to visualize the extent of transferred electron density by application of the extended transition state (ETS) energy decomposition theory in combination with the natural orbitals for the chemical valence (NOCV) model.<sup>9</sup> The ETS-NOCV method provides a compact description of charge rearrangements and corresponding energy contributions from NOCV orbitals to chemical bonds and electronic interactions. According to this model, the molecule of interest is initially divided into fragments in a deliberative manner such that bonding and electronic interactions of interest may be revealed

upon combination of the two fragments back into the original molecule. Electron charge-transfer channels (including both charge inflows (i.e., concentration of electron density) and outflows (i.e., depletion of electron density)) are then exposed via deformation density analysis. Fragmentation of the biphenyl system in our study was best achieved via cleavage of the C--C bond connecting the two aromatic rings. This leads to one of the benzene fragments bearing the electron-donating  $\text{NMe}_2$  group and the other the electron-accepting CHO group. We hoped that upon combination of the two fragments via the ETS-NOCV protocol that the interaction between these two complementary functional groups would be revealed in addition to the expected very strong electronic interaction resulting from formation of the central C--C bond. The result of the calculation is a set of NOCV deformation densities ordered according to their energetic contributions. For compound 2, while the two strongest electronic interactions provided by ETS-NOCV analysis represented formation of the C--C biphenyl bond as anticipated, the third strongest interaction observed included the desired  $n \rightarrow \pi^*$  interaction (Figure 2). The net charge transfer is readily visualized as a dark

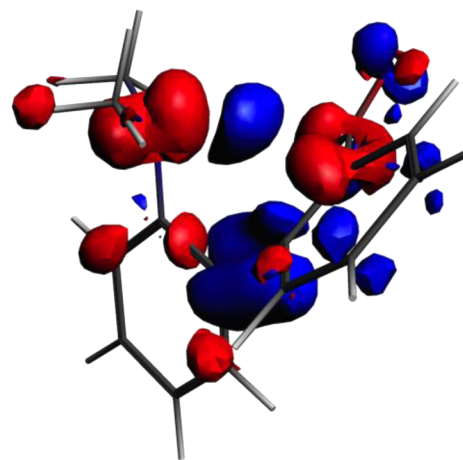


**Figure 2.** Selected deformation density revealing the  $n \rightarrow \pi^*$  interaction as provided by ETS-NOCV (employing the GGA:BP functional with a TZP basis set) analysis of biphenyl 2 (isosurface value = 0.0002). Charge inflows (i.e., concentrations of electron density) are displayed in blue color, and outflows (i.e., depletions of electron density) are displayed in red. The volume of electron density transferred between the nitrogen atom of the  $\text{NMe}_2$  group (on the left) and the  $\pi^*$  of the carbonyl group (on the right) is readily visualized as a blue globule situated directly between the two groups.

blue globule in Figure 2 and is located directly along a line between the nitrogen atom and the carbonyl carbon atom as expected. The nitrogen atom suffers from depletion of electron density (note the red globule about the nitrogen atom on the left in the figure), while the oxygen atom displays a buildup of electron density (blue globule) as expected. The volume of this transferred electron density ( $1.18 \text{ \AA}^3$ ) from the nitrogen to the carbonyl group could be quantified using the Chimera program.<sup>10</sup> Unfortunately, the energy of the  $n \rightarrow \pi^*$  interaction cannot be directly derived from the energy decomposition provided by the ETS-NOCV analysis because we were unable to cleanly separate the  $n \rightarrow \pi^*$  interaction from contaminating residual interactions resulting from C--C bond formation between the two benzene rings as well as from residual



interactions between the aldehyde group and the aromatic  $\pi$  system as observed in Figure 2.

Natural bond orbital (NBO) analysis has been used previously to estimate energetic contributions from donor/acceptor pairs in molecules via second-order perturbative analysis.<sup>2b,4a-c,e,f</sup> We conducted such an analysis on the B3LYP/6-31G(d)-minimized geometry of **2** using a single-point calculation at the B3LYP/6-311+G(2d,p) level of theory. The NBO calculation confirmed the interaction of the nitrogen lone pair with the antibonding orbital of the C=O  $\pi$  bond and corroborated their near-optimal alignment (Figure 3). Second-order perturbation theory provided an estimation for the  $n \rightarrow \pi^*$  interaction energy of 2.12 kcal/mol.

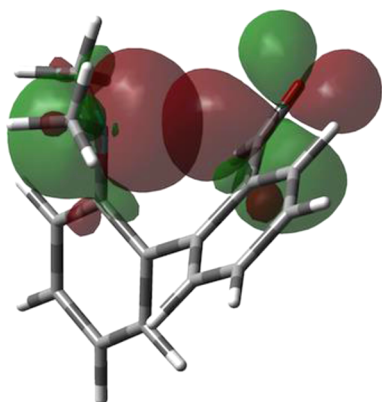
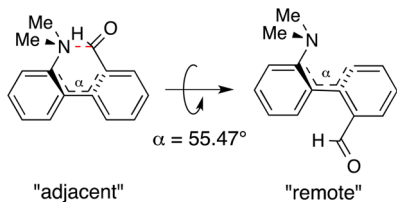


**Figure 3.** NBO analysis of biphenyl **2** with the molecule oriented as in Figure 2A. The interaction between the nitrogen lone pair and the carbonyl group  $\pi^*$  is shown via overlap of the orbitals.

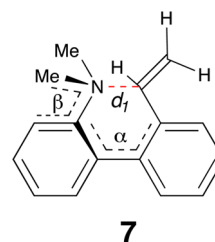
We considered a second method for estimation of the energy of interaction. Starting from the minimized structure of **2**, we rotated the two benzene rings of the biphenyl system about the joining C–C bond until the dihedral angle of the minimized structure was matched, but now where the NMe<sub>2</sub> and CHO groups were directed away from one another (see Scheme 1).

**Scheme 1.** “Adjacent” and “Remote” Conformations for Compound **6**



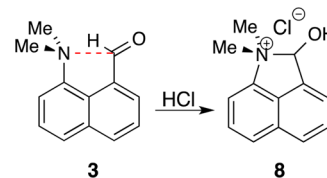
No other structural relaxations were allowed in the system. This new structure will be referred to as the “remote” structure, while the original minimized structure is considered to be “adjacent”. We surmised that except for residual repulsive steric effects between the two interacting groups and the attractive  $n \rightarrow \pi^*$  interaction found in the adjacent structure, all other background contributions would be eliminated upon subtraction of the two energies. A single-point energy calculation was performed on the remote conformation at the B3LYP/6-311+G(2d,p) level. The difference in energies between the optimized adjacent structure of **2** (where the  $n \rightarrow \pi^*$  was active) and the remote model (where the  $n \rightarrow \pi^*$  was no longer possible) was observed to be 1.73 kcal/mol. A correction needs

to be applied to this estimation method, however, since a steric contribution to the adjacent structure, not present in the remote structure, resulting from the proximity of the NMe<sub>2</sub> group to the CHO group is anticipated. We attempted to estimate the cost of this steric effect by studying compound **7**, in which the aldehyde group was replaced by a CH=CH<sub>2</sub> group. In the absence of an electrophilic  $\pi^*$  orbital there is expected to be minimal  $n \rightarrow \pi^*$  delocalization in this case. Additionally, it is expected that steric effects would be minimized upon optimization of the geometry of **7**. We then reoptimized **7** after freezing key structural features to match those of **2** (i.e., the dihedral angles  $\alpha$  (i.e., 55.45°) and  $\beta$  (69.63°), and the N–C distance  $d_1$  (2.957 Å)). In this “partially optimized” geometry of **7**, we expected the steric effects between the two interacting groups to be similar to those of **2** (assuming the distant CH<sub>2</sub> group exerts little effect). The difference in energies between the two structures (i.e., **7** and partially optimized **7**) of 0.51 kcal/mol, therefore, provided an estimate of the steric strain levied by repulsion between the NMe<sub>2</sub> group and the C=C(O) bond. Adding this strain energy to the 1.73 kcal/mol electronic energy obtained previously provides an estimate for the  $n \rightarrow \pi^*$  interaction energy of 2.24 kcal/mol, which is consistent with the 2.12 kcal/mol obtained via NBO analysis. In addition, these estimates for the  $n \rightarrow \pi^*$  stabilization energy are in general agreement with previous estimates of ~1–2 kcal/mol proffered by Allinger.<sup>3</sup>



**2. Structural Consequences of Protonation of the Carbonyl Group of Biphenyl **2**.** Wallis isolated crystals of **8** formed upon protonation of 1-(dimethylamino)naphthalene-8-carboxyaldehyde (**3**, Scheme 2).<sup>5</sup> X-ray crystallographic analysis

**Scheme 2.** Protonation of the Carbonyl Group of **3** To Form Ring-Closed **8**



revealed that a bond between the NMe<sub>2</sub> nitrogen atom and the carbon of the carbonyl group was nearly fully formed. Similar to this experimental observation, upon in silico protonation of the carbonyl group of **2**, a bond was formed between the nitrogen atom and the carbon of the carbonyl group to afford **9** (Figure 4). The N–C bond length of 1.588 Å is shorter than the experimental length found in Wallis’s compound **8** (1.638 Å)<sup>5b</sup> indicating a more fully developed bond, probably due to the greater flexibility of the biphenyl backbone relative to that of naphthalene. Similarly, the C–O bond length in **9** was determined to be 1.382 Å, which is considerably longer than that of neutral **2** (1.218 Å) and also slightly longer than that observed in **8** (1.353 Å), indicating a nearly fully severed  $\pi$

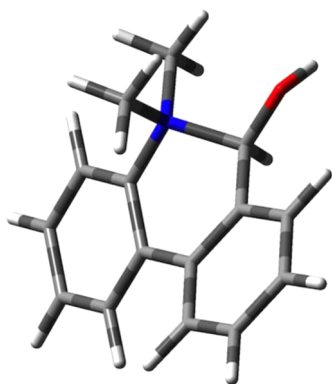
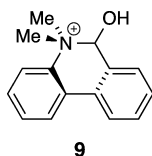


**Figure 4.** Geometry of compound **9** as minimized at the B3LYP/6-31G(d) level of theory.

bond. Finally, unlike neutral **2**, the carbon of the carbonyl group exhibits significant pyramidalization. Formation of an N–C bond under these conditions is consistent with the charge transfer interaction observed in neutral **2** representing an early stage along the trajectory of bond formation between the two groups.



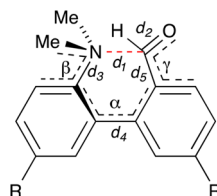
### 3. Computational Analysis of 5- and 5'-Substituted 2-(Dimethylamino)biphenyl-2'-carboxaldehydes (**6**).

*a. Structural and Electronic Effects Resulting from Substitution at the 5'-Position of the CHO-Bearing Ring.* We surmised that substitution on the biphenyl rings with electron-donating or electron-withdrawing groups should affect the extent of interaction between the two groups and possibly portray various stages of bond formation between the nucleophilic nitrogen atom and the electrophilic carbonyl group. As mentioned previously, electron-withdrawing groups (characterized by positive  $\sigma_p$ -Hammett constants) positioned *para* to the aldehyde carbonyl group are expected to promote additional charge transfer between the two groups, while electron-donating groups (characterized by negative  $\sigma_p$ -Hammett constants) should discourage such interaction. The range of substituents examined is provided in Table 2 (entries 1–10) along with relevant structural data for the minimized structures. As before, all geometry minimizations were conducted at the B3LYP/6-31G(d) level of theory. As can be seen from columns 4 and 9 in Table 2, there is a clear correlation between the electronic effects exerted by substituents and the extent to which the NMe<sub>2</sub> group is comfortable in its interactions with the carbonyl  $\pi^*$  orbitals. As the electron-withdrawing nature of the substituent increases (see entries 1–6) the nitrogen atom is drawn increasingly closer to the carbonyl carbon atom, decreasing both the N–C interatomic distance ( $d_1$ ) and the resulting dihedral angle between the biphenyl rings ( $\alpha$ ). Furthermore, the degree of pyramidalization of the carbonyl group, as measured by  $\Theta$  (column 12), was observed to increase. In concert with the increased pyramidalization, the dihedral angle describing the spatial relationship of the carbonyl group with regards to the aromatic ring to which it is attached ( $\gamma$ , column 11) also increased. With loss of conjugation between the carbonyl and

aromatic  $\pi$  systems, a gradual lengthening of the C–C bond between the aldehyde group and the benzene ring ( $d_5$ , column 8) was also observed. As for the interacting NMe<sub>2</sub> group, as the electron-withdrawing character of the substituent on the CHO-bearing ring increased, more effective donation of the nitrogen lone pair into the  $\pi^*$  orbital of the carbonyl group exhibited the following effects: (i) the nitrogen atom increasing turned opportunistically toward the carbonyl carbon as measured by the dihedral angle  $\beta$  (i.e., the dihedral angle became shallower), (ii) there was a slight trend toward a more tetrahedral geometry about the nitrogen atom of the NMe<sub>2</sub> group (as measured by the average angle about the nitrogen atom, column 13) as its lone pair was increasingly used to interact with the carbonyl group and less for resonance interaction with the aromatic ring to which it is attached, and (iii) there was a corresponding increase in C–N bond length ( $d_3$ ) between the aromatic ring and the NMe<sub>2</sub> group in accord with the loss of resonance interaction. Variation of the length of the C–C bond tethering the two aromatic rings ( $d_4$ ) changed subtly with dihedral angle  $\alpha$ . With decreasing  $\alpha$ , resonance interaction between the two rings is enhanced, and a commensurate decrease in bond length was observed. Substitution on the CHO-bearing ring by electron-donating groups, on the other hand (see entries 6–10), resulted in expected trends in the direction opposite to substitution with electron-withdrawing groups for all of the structural parameters. Most significantly, there was observed a regular increase in  $d_1$  and dihedral angle  $\alpha$  and lessening of the degree of pyramidalization of the carbonyl group ( $\Theta$ ). A plot of the Hammett constants for the substituents ( $\sigma_p$ ) versus  $d_1$  afforded a strong linear correlation ( $R^2 = 0.98$ , Figure 5A).

Curiously, however, and unlike the other parameters, the C=O bond length (Table 2, column 5) appeared to behave contrary to expectations. We expected that with increased  $n \rightarrow \pi^*$  interactions the C=O bond would lengthen in reaction to occupation of the  $\pi^*$  orbital by the lone pair electrons. Surprisingly, what was actually observed was a shortening of the C=O bond length. However, the length of the C=O bond is also significantly impacted by conjugative interactions with the aromatic ring. Decreasing electron density in the ring will tend to shorten the C=O bond via decreased resonance interaction.<sup>12</sup> Thus, the two electronic effects are at odds with one another. The presence of electron-withdrawing groups on the CHO-bearing ring should result in lengthening of the C=O bond length via enhanced  $n \rightarrow \pi^*$  interactions, but also work to shorten the bond length due to decreased resonance interaction with the aromatic ring. It would appear that the resonance effect dominates, presumably because of the relative weakness of the  $n \rightarrow \pi^*$  interaction.

Finally, calculated atomic charges (CHelpG charges calculated at the B3LYP/6-311+G(2d,p) level) on the nitrogen atom of the NMe<sub>2</sub> group and the carbon of the carbonyl group (see Supporting Information Table S1) were found to be much less useful and informative than the structural data. It might be expected that greater  $n \rightarrow \pi^*$  interactions would lead to decreasing negative charge on the electron-rich nitrogen atom as its lone pair is increasingly donated into the  $\pi^*$  orbital as well as decreased positive charge on the carbonyl carbon atom as it accepts the electron density. However, the average charge on the nitrogen atom for all of the derivatives was determined to be  $-0.13$ , deviated by less than  $\pm 0.03$ , and exhibited no obvious trend in the direction of change of value. Likewise, the charge on the carbonyl carbon was  $+0.44$  and similarly deviated randomly by less than  $\pm 0.03$ .

Table 2. Calculated Structural Data for Optimized Structures 6<sup>a</sup>


entry	R <sup>b</sup>	R' <sup>b</sup>	d <sub>1</sub> (Å)	d <sub>2</sub> (Å)	d <sub>3</sub> (Å)	d <sub>4</sub> (Å)	d <sub>5</sub> (Å)	α <sup>c</sup> (deg)	β <sup>c</sup> (deg)	γ <sup>c</sup> (deg)	Θ <sup>d</sup> (deg)	avg ∠ <sub>N</sub> <sup>e</sup> (deg)
1	H	NO <sub>2</sub>	2.836	1.217	1.425	1.492	1.494	51.90	109.74	14.96	3.20	114.68
2	H	CN	2.885	1.217	1.424	1.493	1.493	53.48	110.62	13.66	2.83	114.68
3	H	CF <sub>3</sub>	2.891	1.217	1.423	1.493	1.492	53.46	110.81	13.64	2.83	114.74
4	H	Cl	2.952	1.218	1.422	1.494	1.488	55.21	112.03	11.76	2.36	114.80
5	H	F	2.957	1.218	1.423	1.494	1.488	55.45	112.03	11.85	2.36	114.82
6	H	H	2.958	1.218	1.423	1.494	1.488	55.45	112.03	11.85	2.36	114.82
7	H	CH <sub>3</sub>	2.978	1.219	1.423	1.494	1.485	55.85	112.71	11.18	2.21	114.88
8	H	OH	3.014	1.220	1.422	1.495	1.481	56.83	113.17	9.82	2.02	114.91
9	H	NH <sub>2</sub>	3.070	1.221	1.420	1.496	1.477	58.51	114.64	8.22	1.69	115.05
10	H	NMe <sub>2</sub>	3.071	1.222	1.420	1.497	1.475	58.29	115.13	7.85	1.64	115.16
11	NO <sub>2</sub>	H	3.034	1.217	1.405	1.495	1.488	56.44	121.94	12.11	1.93	116.16
12	CN	H	3.015	1.217	1.410	1.495	1.488	56.42	118.75	11.95	2.02	115.67
13	CF <sub>3</sub>	H	2.994	1.218	1.416	1.495	1.488	56.16	116.64	11.85	2.11	115.31
14	Cl	H	2.960	1.218	1.421	1.494	1.489	55.51	112.56	12.11	2.30	114.90
15	F	H	2.938	1.218	1.425	1.494	1.489	55.18	110.15	12.12	2.40	114.66
16	CH <sub>3</sub>	H	2.949	1.218	1.424	1.494	1.488	55.18	117.71	11.79	2.40	114.71
17	OH	H	2.920	1.218	1.428	1.494	1.488	54.82	108.01	12.07	2.49	114.47
18	NH <sub>2</sub>	H	2.915	1.219	1.430	1.494	1.488	54.80	106.60	11.71	2.54	114.35
19	NMe <sub>2</sub>	H	2.914	1.219	1.430	1.494	1.488	54.64	107.38	11.75	2.54	114.35
20	NMe <sub>2</sub>	NO <sub>2</sub>	2.769	1.217	1.432	1.492	1.495	50.41	103.75	15.37	3.76	114.30
21	NO <sub>2</sub>	NMe <sub>2</sub>	3.131	1.222	1.400	1.498	1.474	58.41	126.37	8.48	1.40	116.79

<sup>a</sup>Geometry minimizations were carried out at the DFT B3LYP/6-31G(d) level of theory. Corresponding energies and coordinates are provided in the Supporting Information. <sup>b</sup>Hammett  $\sigma_p$  values: NO<sub>2</sub>, 0.78; CN, 0.66; CF<sub>3</sub>, 0.54; Cl, 0.23; F, 0.06; H, 0.0; CH<sub>3</sub>, -0.17; OH, -0.37; NH<sub>2</sub>, -0.66; NMe<sub>2</sub>, -0.83.<sup>11</sup> <sup>c</sup>α, β, and γ are the dihedral angles defined by the atoms in the accompanying graphic. <sup>d</sup>The angle Θ is defined in Table 1. <sup>e</sup>The average of the angles centered about the nitrogen atom of the interacting NMe<sub>2</sub> group.

In addition to the structural changes that resulted from substitution on the CHO-bearing ring, we also probed (see Table 3, entries 1–10) the electronic and energetic impact that various substituents exerted on the n→π\* interactions by examination of: (i) second-order perturbation energies as provided by NBO analysis ( $E_{\text{SOP}}$ , column 4), (ii) the volume of electron density transferred from the nitrogen atom of the NMe<sub>2</sub> group to the π\* orbital of the carbonyl group as provided by ETS-NOCV analysis (performed in the same manner for all of the derivatives as was described earlier for compound 2) and quantified using Chimera ( $V(\rho)$ , column 5), and (iii) the difference in energies between “adjacent” and “remote” conformations of the variously substituted biphenyls as described in Scheme 1 ( $\Delta E_{\text{conf}}$ , column 6).

As expected, the strength of the n→π\* interactions increased in unison with the electron-withdrawing or electron-donating nature of the substituents (Table 3, entries 1–10). The  $E_{\text{SOP}}$  values correlated reasonably well with the substituent  $\sigma_p$  values (Figure 5B,  $R^2 = 0.94$ ). A similarly strong correlation was observed between ETS-NOCV  $V(\rho)$  and  $\sigma_p$  values (Figure 5C,  $R^2 = 0.96$ ). Notice that substitution with the particularly strong electron-donating NH<sub>2</sub> and NMe<sub>2</sub> groups was sufficient to completely inhibit charge transfer (i.e.,  $V(\rho) = 0$ ) according to ETS-NOCV analysis even though NBO analysis suggested much weaker, but continued, orbital interactions. Correlation with  $\Delta E_{\text{conf}}$  was the weakest (Figure 5D,  $R^2 = 0.88$ ), rendering

this method for probing n→π\* interactions to be generally unsatisfactory except, perhaps, in a qualitative sense.

**b. Structural and Electronic Effects Resulting from Substitution at the 5-Position of the NMe<sub>2</sub>-Substituted Ring.** We expected that substitution on the benzene ring bearing the NMe<sub>2</sub> group would generally exhibit an effect opposite to that observed for identical substitution on the ring bearing the aldehyde group. Electron-donating groups should enhance the ability of the nitrogen atom to transfer electron density into the carbonyl π\* orbital, while electron-withdrawing groups should inhibit such interaction. The relevant structural data pertaining to such substitutions at position R of compound 6 are compiled in Table 2 (entries 11–19). As with substitution at the R' position, the expected trends are indeed generally observed. Electron-donating groups appear to increase the extent of interaction between the nitrogen lone pair and the carbonyl π\* orbital as evidenced by shortening of the N–C distance ( $d_1$ ), tightening of the dihedral angle between the two biphenyl rings, and increase in carbonyl group pyramidalization (Θ). Unlike substitution on the CHO-bearing ring, however, the correlation between  $\sigma_p$  and  $d_1$  is far from linear, and segmented behavior is observed (Figure 6A). While electron-withdrawing groups appear to exert a regular effect upon  $d_1$  (local  $R^2 = 0.99$ ) the three electron-donating groups NMe<sub>2</sub>, NH<sub>2</sub>, and OH are nearly equivalent in their effect. It appears that beyond OH, increased electron-donating character of the substituent is unable to further enhance the n→π\* interaction

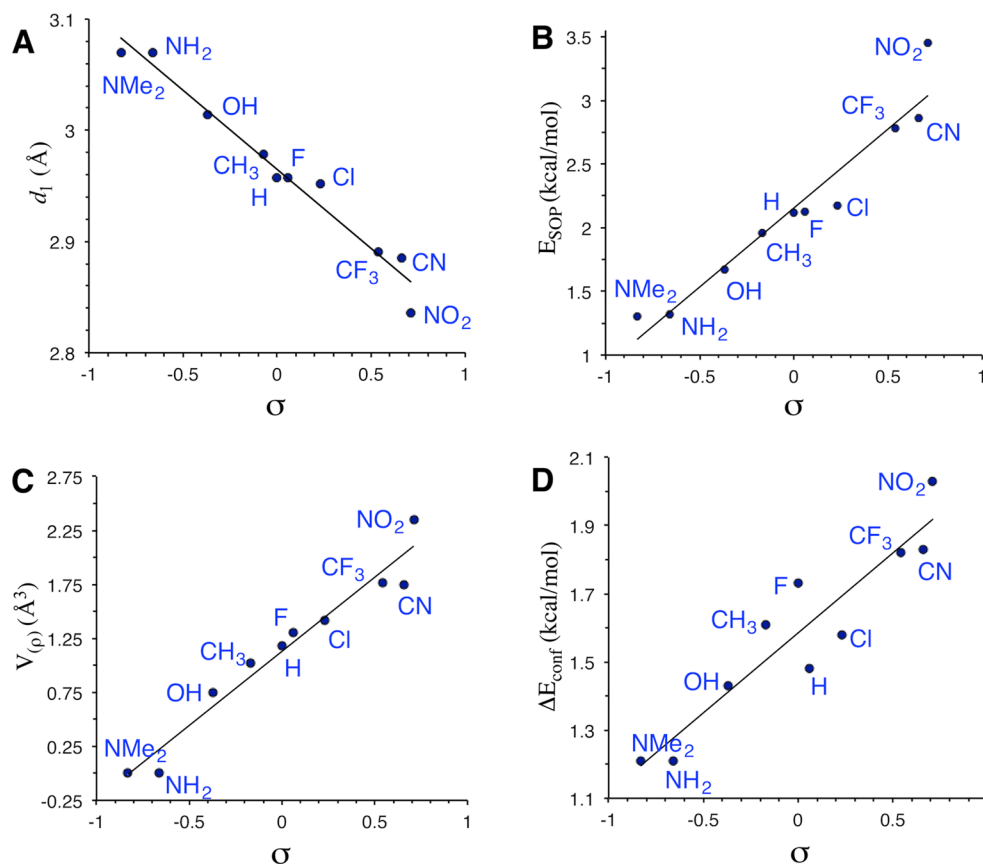


**Figure 5.** Plots of Hammett  $\sigma_p$  values (substituent  $R'$  in **6**) versus relevant structural and electronic features: (A) N–C interatomic distances; (B) second-order perturbation energies for the  $n \rightarrow \pi^*$  interaction between the nitrogen lone pair and carbonyl group from NBO analysis; (C) volume of electron density transferred via the  $n \rightarrow \pi^*$  interaction as obtained by ETS–NOCV analysis; (D) difference in energies (B3LYP/6-311+G(2d,p)) between the “adjacent” and “remote” conformations of **6** (see Scheme 1).

(vide infra). The other structural parameters provided in Table 2, with the exception of the bond length  $d_5$  and dihedral angle  $\gamma$ , behave in a manner commensurate with the arguments presented earlier for substitution on the aldehyde ring. Unlike what was observed upon substitution on the CHO-bearing ring, the C–C bond length  $d_5$  remained essentially constant upon substitution on the NMe<sub>2</sub>-bearing ring with both electron-withdrawing and electron-donating substituents. The observed length (1.488 Å) was essentially equivalent to that of unsubstituted **2** (i.e., when  $R' = H$  in both cases). Similarly, the dihedral angle  $\gamma$  for the derivatives appeared to stagnate at a value of  $\sim 12^\circ$  which, again, is close to the value calculated for unsubstituted **2** ( $11.85^\circ$ ).

The electronic and energetic impacts of substitution on the NMe<sub>2</sub>-bearing ring on the resulting  $n \rightarrow \pi^*$  interactions are compiled in Table 3 (entries 11–19). As with the correlation between  $\sigma_p$  and  $d_1$ , nonlinear and segmented behavior is also observed in the attempted correlation of  $\sigma_p$  with  $E_{SOP}$  (Figure 6B). Substitution by electron-withdrawing groups exhibits a strong correlation with  $\sigma_p$  (local  $R^2 = 1.00$ ); flattened behavior is observed with the stronger electron-donating groups, and disjointed behavior is again observed with  $R = CH_3$  or H. Attempted correlation of  $\sigma_p$  with the volumes of electron density transfer ( $V(p)$ ) provided by ETS–NOCV analysis (Figure 6C) resulted in even greater isolated behavior. While the drop in transferred electron density is precipitous upon substitution by strong electron-withdrawing groups, and a flattened correlation is observed with the electron donor

groups, rather chaotic behavior is observed for  $R = CH_3$ , H, F, and Cl. Curiously, an attempt to utilize the difference in energies between the open and closed conformations of these variously substituted biphenyls to probe the energy of the  $n \rightarrow \pi^*$  proved to be worthless for this series of compounds (Figure 6D) confirming this proposed method to be unreliable.

The shortest N–C interatomic distance obtained by positioning a strong electron-donating group (NMe<sub>2</sub>) on the NMe<sub>2</sub>-bearing ring (2.914 Å corresponding to a dihedral angle between the biphenyl rings of  $54.64^\circ$ ) was still longer than the shortest distance (2.836 Å, dihedral angle =  $51.90^\circ$ ) obtained by positioning a strong electron-withdrawing group (NO<sub>2</sub>) onto the CHO-bearing ring. Accordingly, the difference between the shortest and longest distances ( $\Delta d_1$ ) obtained by altering the substituents on the NMe<sub>2</sub>-bearing ring (0.12 Å) was also only half that obtained by altering the substituents on the CHO-bearing ring (0.23 Å). The difference between the greatest and least volumes of transferred electron density (i.e.,  $\Delta V(p)$ ) observed by altering the substituents on the NMe<sub>2</sub>-bearing ring ( $1.66 \text{ Å}^3$ ) was considerably less than that observed upon altering the substituents on the CHO-bearing ring ( $2.35 \text{ Å}^3$ ). Finally, the  $n \rightarrow \pi^*$  interaction energies obtained via NBO analysis spanned a larger range for substitutions on the CHO-substituted ring (2.15 kcal/mol) than they did for the NMe<sub>2</sub>-substituted ring (1.04 kcal/mol). All of these observations indicate that, at least for this series of compounds, there is a greater sensitivity of  $n \rightarrow \pi^*$  interactions toward the electrophilic properties of the CHO group than the nucleophilic character of



Table 3. Calculated Electronic and Energetic Data for Optimized Structures 6

entry	R	R'	$E_{\text{SOP}}^a$ (kcal/mol)	$V(\rho)^b$ (Å <sup>3</sup> )	$\Delta E_{\text{conf}}^c$ (kcal/mol)
1	H	NO <sub>2</sub>	3.45	2.35	2.03
2	H	CN	2.86	1.75	1.83
3	H	CF <sub>3</sub>	2.78	1.77	1.82
4	H	Cl	2.17	1.42	1.58
5	H	F	2.13	1.30	1.48
6	H	H	2.12	1.18	1.73
7	H	CH <sub>3</sub>	1.96	1.02	1.58
8	H	OH	1.67	0.75	1.43
9	H	NH <sub>2</sub>	1.32	0.0	1.21
10	H	NMe <sub>2</sub>	1.30	0.0	1.21
11	NO <sub>2</sub>	H	1.48	0.0	1.97
12	CN	H	1.63	0.52	1.87
13	CF <sub>3</sub>	H	1.80	0.89	1.93
14	Cl	H	2.10	1.34	1.95
15	F	H	2.29	1.48	2.02
16	CH <sub>3</sub>	H	2.21	1.38	1.67
17	OH	H	2.46	1.58	2.08
18	NH <sub>2</sub>	H	2.52	1.65	1.97
19	NMe <sub>2</sub>	H	2.55	1.66	1.81
20	NMe <sub>2</sub>	NO <sub>2</sub>	4.51	2.51	
21	NO <sub>2</sub>	NMe <sub>2</sub>	0.94	0.0	

<sup>a</sup>The  $n \rightarrow \pi^*$  interaction energy provided by second order perturbation theory analysis of donor–acceptor interactions from within NBO.

<sup>b</sup>The calculated volume of electron density transferred as provided by ETS-NOCV analysis and computed by Chimera (surface isovalue = 0.0002). <sup>c</sup>Difference in energies between the “adjacent” and “remote” conformations of the respective biphenyl compounds (see Scheme 1).

the NMe<sub>2</sub> group. This is most likely due to the requirement for the nitrogen atom lone pair to be directed away from effective conjugation with the aromatic  $\pi$  system and toward the carbonyl group in order to engage in the  $n \rightarrow \pi^*$  interaction. Since substituent effects on the NMe<sub>2</sub>-bearing ring are most efficiently transmitted to the NMe<sub>2</sub> group via such resonance effects, rotation of the lone pair away from conjugation attenuates the substituents' effectiveness. The carbonyl group, on the other hand, deviates only slightly from planarity with respect to the aromatic ring (the maximum value for  $\gamma$  = 14.96°), allowing largely for retention of conjugation and continued effective transmission of substituent effects. This theory is supported by the “plateauing” effect observed upon substitution on the NMe<sub>2</sub>-bearing ring with R = NMe<sub>2</sub>, NH<sub>2</sub>, and OH in Figure 6a–c. Beyond rotation of the nucleophilic NMe<sub>2</sub> group out of the plane of the aromatic ring as measured by  $\beta \sim 108^\circ$  (for R = OH), resonance effects are more or less stagnated and the electron-donating ability of the substituent is essentially saturated.

*c. Structural and Electronic Effects Resulting from Bis-substitution at the 5,5'-Positions of the Biphenyl System.* Given the results described above for substitution on either the NMe<sub>2</sub>-bearing aromatic ring or the CHO-bearing ring, we thought it worthwhile to consider the two possible extremes of substitution on both rings simultaneously. On the basis of the observations discussed earlier for the singly substituted molecules, placement of the very strong electron-donating NMe<sub>2</sub> group onto the NMe<sub>2</sub>-bearing ring in addition to placement of the strong electron-withdrawing NO<sub>2</sub> group onto the CHO-bearing ring was expected to result in maximum  $n \rightarrow \pi^*$  interactions (Tables 2 and 3, entry 20). Indeed, the

minimized structure for this compound afforded the shortest observed interatomic C–N distance of 2.769 Å, a tight biphenyl dihedral angle of 50.41°, and a maximum degree of carbonyl group pyramidalization (3.76°). Additionally, the NBO second-order perturbation energy estimate for the interaction of 4.51 kcal/mol surpassed all other interaction energies we had observed for this class of compound. This was coupled with the largest measured volume of transferred electron density as well (2.51 Å<sup>3</sup>). Interestingly, however, the C=O bond length ( $d_2$ ) still failed to deviate significantly from the  $\sim 1.22$  Å measurement. This observation highlights the reluctance of the molecule to engage in more complete bond formation that would require build up of significant atomic charges on its way to formation of a zwitterionic addition product, at least in silico. We tested this potential limitation by computationally investigating compound **5a** that has been demonstrated, via X-ray crystallography, to adopt a zwitterionic structure through formation of a nearly complete N–C bond (although solution-phase NMR studies demonstrated that a solvent-dependent equilibrium was established between the ring-open and ring-closed structures).<sup>2d</sup> A model of **5a** was initially constructed to incorporate the key bond lengths, interatomic distances, and torsion angles reported for the ring-closed crystal structure. Upon computational minimization of the starting structure, however, the N–C bond slowly increased in length and eventually ruptured, and the C=C bond was, in turn, reformed. The resulting structure was essentially identical to the structure obtained via minimization of the biphenyl system in the absence of an initially formed N–C bond. Running the computations including implicit solvation (methanol) did not prevent the N–C bond cleavage from occurring. This finding highlights the importance of experimentally investigating the behavior of compounds engaged in weak  $n \rightarrow \pi^*$  interactions and not relying solely upon computational results.

At the other extreme, placing the strong electron-donating NMe<sub>2</sub> group onto the CHO-bearing ring in conjunction with the NO<sub>2</sub> group on the NMe<sub>2</sub>-bearing ring (i.e., Tables 2 and 3, entry 22) resulted in the two groups repelling one another to afford the greatest measured interatomic N–C distance of 3.13 Å and the least pyramidalized carbonyl group ( $\Theta$  = 1.4°) of all the derivatives studied. In addition, the lowest NBO interaction energy of 0.94 kcal/mol was observed.

## CONCLUSIONS

From the studies described above, 5'-substituted-2-(dimethylamino)biphenyl-2'-carboxaldehydes appear to be a promising strategic framework for locating points along the Bürgi–Dunitz trajectory for N–C bond formation between an NMe<sub>2</sub> and C=O group. Of particular interest is the sensitivity of the N–C interatomic distance to the nature of the substituent positioned *para* to the C=O aldehyde group. Electron-withdrawing groups clearly drew the nitrogen atom closer to the carbon of the C=O bond in a regular manner via constriction of the dihedral angle between the two phenyl rings, while electron-donating groups pushed the two atoms apart (Table 2). A strong correlation with the substituent's Hammett constants was determined. That the interaction derives from a charge transfer mechanism was corroborated by ETS-NOCV studies where a strong correlation between increasing volumes of transferred electron density and shorter N–C interatomic distances may be observed (Figure 7A,  $R^2$  = 0.98). A similarly strong correlation between the  $n \rightarrow \pi^*$  interaction energies as



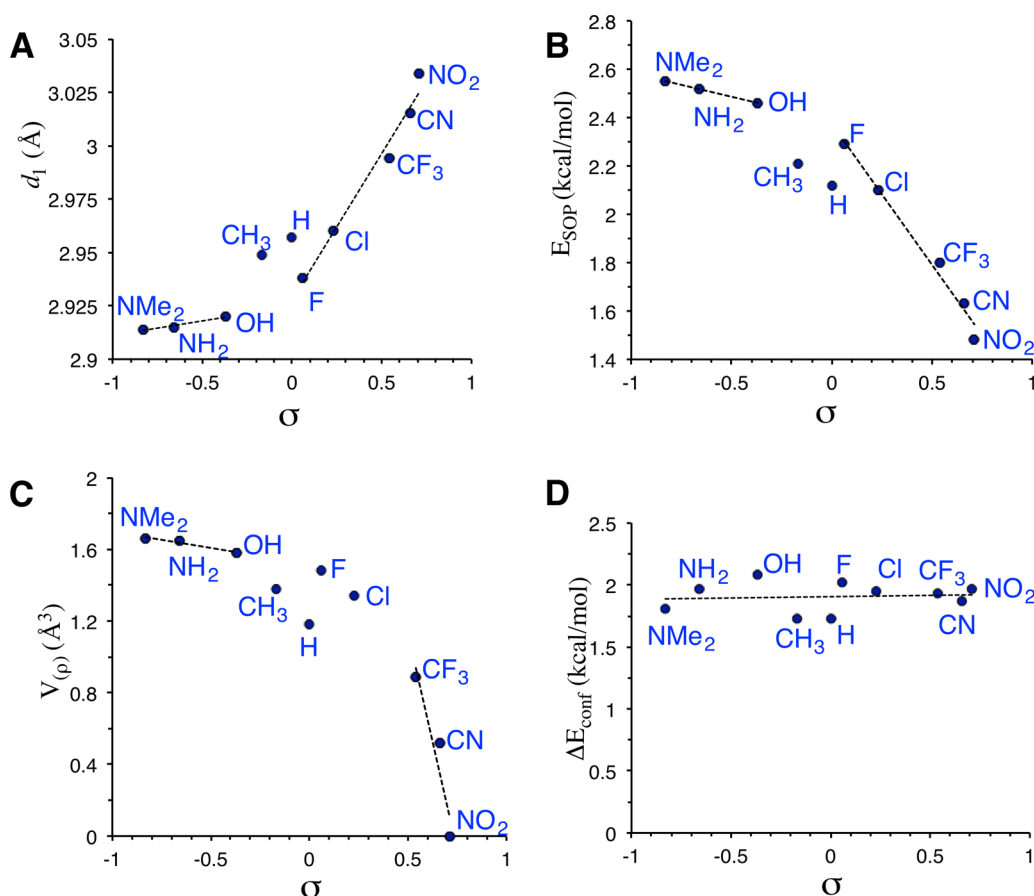


**Figure 6.** Correlations of Hammett  $\sigma_p$  values (substituent R in **6**) with relevant structural and electronic features: (A) N–C interatomic distances; (B) second-order perturbation energies for the  $n \rightarrow \pi^*$  interaction between the nitrogen lone pair and carbonyl group from NBO analysis; (C) volume of electron density transferred via the  $n \rightarrow \pi^*$  interaction as obtained by ETS-NOCV analysis; (D) difference in energies (B3LYP/6-311+G(2d,p)) between the adjacent and remote conformations of **6**.

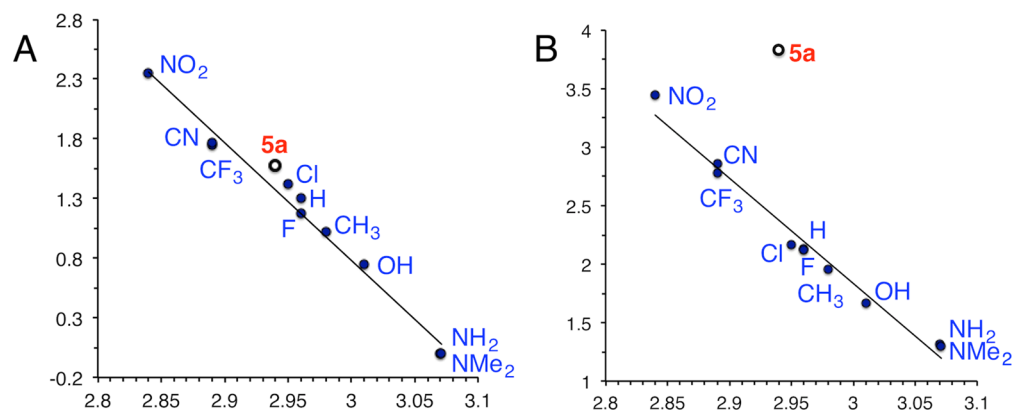


**Figure 7.** Correlations of N–C interatomic distances (varying substituent R' in **6**) with (A) volume of electron density transferred via the  $n \rightarrow \pi^*$  interaction as obtained by ETS-NOCV analysis; (B) second-order perturbation energies for the  $n \rightarrow \pi^*$  interaction between the nitrogen lone pair and carbonyl group from NBO analysis.

derived from NBO second-order perturbation analysis and N–C interatomic distances was obtained (Figure 7B,  $R^2 = 0.98$ ).

Compound **5a** provided an example of a compound that is known, at least in the crystalline phase, to form a nearly complete N–C bond. However, our computational studies were unable to replicate that finding highlighting the limitations of computations at this level of theory to reproduce the experimental results, at least where zwitterionic structures are involved. NBO analysis of the computationally optimized

structure for **5a** (i.e., for which the N–C bond is not formed) provided a second-order perturbation energy for the  $n(\text{N}) \rightarrow \pi^*(\text{C}=\text{C})$  interaction of 3.83 kcal/mol at an interatomic distance of 2.938 Å, which lies far from the trendline of Figure 7B. However, it is unrealistic to expect that the energies of interaction of the nitrogen lone pair with a  $\text{C}=\text{C}$  bond should be related to that of a  $\text{C}=\text{O}$  bond. Interestingly, however, ETS-NOCV analysis of compound **5a** provided a volume of electron density transfer of 1.58 Å<sup>3</sup>, which fits quite nicely on

the trendline in Figure 7A (resulting  $R^2 = 0.98$ ). ETS-NOCV analysis, therefore, appears to be an excellent predictor of the extent of  $n \rightarrow \pi^*$  interactions. If so, then those 5'-substituted biphenyls with electron density transfer volumes of  $\sim 1.6 \text{ \AA}^3$  or greater (i.e., substituents *para* to the aldehyde group =  $\text{CF}_3$ ,  $\text{CN}$ ,  $\text{NO}_2$ ) might be expected to exhibit nearly, or (especially for  $\text{NO}_2$ ) possibly complete N–C bond formation in the crystal structure and perhaps in solution. Other substitutions, especially when  $R = \text{Cl}$  or  $\text{F}$ , could potentially yield structures of intermediate bond formation. We intend to test this theory by synthesizing this series of compounds and analyzing their structures by X-ray crystallography, IR spectroscopy, and  $^1\text{H}$ ,  $^{13}\text{C}$ , and  $^{15}\text{N}$  NMR spectroscopy.

## ■ COMPUTATIONAL METHODS

Geometry optimizations and single-point energy calculations were carried out with the Gaussian 09 suite of programs using the B3LYP hybrid functional with the 6-31G(d) (optimizations) and 6-311+G-(2d,p) (single-point calculations) basis sets.<sup>6</sup> Reported energies are uncorrected. Vibrational frequency calculations were carried out on all optimized geometries to confirm them as minima (i.e., no imaginary frequencies). NBO calculations were carried out from within Gaussian 09 employing NBO 3.1 at the B3LYP/6-311+G(2d,p) level of theory. ETS-NOCV calculations were carried out from within the ADF molecular modeling suite employing the GGA:BP functional with a TZP basis set.<sup>13</sup> A consistent isovalue of 0.0002 was applied when generating the NOCV deformation density surfaces. UCSF's Chimera program<sup>10</sup> was employed to quantify the extent of transferred electron density (i.e.,  $V(\rho)$ ) resulting from  $n \rightarrow \pi^*$  interactions as provided by the ETS-NOCV calculations (see the Supporting Information).

## ■ ASSOCIATED CONTENT

### ● Supporting Information

Cartesian coordinates and energies for all newly reported structures, Table S1 containing calculated atomic charges, and the procedure used for quantifying  $V(\rho)$  using Chimera. The Supporting Information is available free of charge on the ACS Publications website at DOI: 10.1021/acs.joc.5b00766.

## ■ AUTHOR INFORMATION

### Corresponding Author

\*E-mail: gbreton@berry.edu.

### Notes

The authors declare no competing financial interest.

## ■ REFERENCES

- (1) (a) Bürgi, H. B.; Dunitz, J. D.; Shefter, E. *Nature New Bio.* **1973**, *244*, 186–188. (b) Bürgi, H. B.; Dunitz, J. D.; Shefter, E. *J. Am. Chem. Soc.* **1973**, *95*, 5065–5067.
- (2) (a) Choudhary, A.; Newberry, R. W.; Raines, R. T. *Org. Lett.* **2014**, *16*, 3421–3423. (b) Newberry, R. W.; Raines, R. T. *ACS Chem. Biol.* **2014**, *9*, 880–883. (c) Lari, A.; Pitak, M. B.; Coles, S. J.; Bresco, E.; Belser, P.; Beyeler, A.; Pilkington, M.; Wallis, J. D. *CrystEngComm* **2011**, *13*, 6978–6984. (d) O'Leary, J.; Wallis, J. D. *Org. Biomol. Chem.* **2009**, *7*, 225–228. (e) O'Leary, J.; Formosa, X.; Skranc, W.; Wallis, J. D. *Org. Biomol. Chem.* **2005**, *3*, 3273–3283. (f) O'Leary, J.; Wallis, J. D.; Wood, M. L. *Acta Crystallogr., Sect. C: Cryst. Struct. Commun.* **2001**, *C57*, 851–853. (g) Crasto, C. J.; Stevens, E. D. *J. Mol. Struct.: THEOCHEM* **1998**, *454*, 51–59.
- (3) Allinger, N. L. *Molecular Structure: Understanding Steric and Electronic Effects from Molecular Mechanics*; Wiley: Hoboken, 2010.
- (4) (a) Newberry, R. W.; Bartlett, G. J.; VanVeller, B.; Woolfson, D. N.; Raines, R. T. *Protein Sci.* **2014**, *23*, 284–288. (b) Bartlett, G. J.; Newberry, R. W.; VanVeller, B.; Raines, R. T.; Woolfson, D. N. *J. Am. Chem. Soc.* **2013**, *135*, 18682–18688. (c) Newberry, R. W.; VanVeller, B.; Guzei, I. A.; Raines, R. T. *J. Am. Chem. Soc.* **2013**, *135*, 7843–7846. (d) Fufezan, C. *Proteins: Struct., Funct., Genet.* **2010**, *78*, 2831–2838. (e) Jakobsche, C. E.; Choudhary, A.; Miller, S. J.; Raines, R. T. *J. Am. Chem. Soc.* **2010**, *132*, 6651–6653. (f) Choudhary, A.; Gandla, D.; Krow, G. R.; Raines, R. T. *J. Am. Chem. Soc.* **2009**, *131*, 7244–7246.
- (5) (a) Mercadal, N.; Day, S. P.; Jarmyn, A.; Pitak, M. B.; Coles, S. J.; Wilson, C.; Rees, G. J.; Hanna, J. V.; Wallis, J. D. *CrystEngComm* **2014**, *16*, 8363–8374. (b) Lari, A.; Pitak, M. B.; Coles, S. J.; Rees, G. J.; Day, S. P.; Smith, M. E.; Hanna, J. V.; Wallis, J. D. *Org. Biomol. Chem.* **2012**, *10*, 7763–7779.
- (6) Gaussian 09, Revision C.01: Frisch, M. J.; Trucks, G. W.; Schlegel, H. B.; Scuseria, G. E.; Robb, M. A.; Cheeseman, J. R.; Scalmani, G.; Barone, V.; Mennucci, B.; Petersson, G. A.; Nakatsuji, H.; Caricato, M.; Li, X.; Hratchian, H. P.; Izmaylov, A. F.; Bloino, J.; Zheng, G.; Sonnenberg, J. L.; Hada, M.; Ehara, M.; Toyota, K.; Fukuda, R.; Hasegawa, J.; Ishida, M.; Nakajima, T.; Honda, Y.; Kitao, O.; Nakai, H.; Vreven, T.; Montgomery, J. A., Jr.; Peralta, J. E.; Ogliaro, F.; Bearpark, M.; Heyd, J. J.; Brothers, E.; Kudin, K. N.; Staroverov, V. N.; Kobayashi, R.; Normand, J.; Raghavachari, K.; Rendell, A.; Burant, J. C.; Iyengar, S. S.; Tomasi, J.; Cossi, M.; Rega, N.; Millam, J. M.; Klene, M.; Knox, J. E.; Cross, J. B.; Bakken, V.; Adamo, C.; Jaramillo, J.; Gomperts, R.; Stratmann, R. E.; Yazyev, O.; Austin, A. J.; Cammi, R.; Pomelli, C.; Ochterski, J. W.; Martin, R. L.; Morokuma, K.; Zakrzewski, V. G.; Voth, G. A.; Salvador, P.; Dannenberg, J. J.; Dapprich, S.; Daniels, A. D.; Farkas, Ö.; Foresman, J. B.; Ortiz, J. V.; Cioslowski, J.; Fox, D. J. Gaussian, Inc., Wallingford, CT, 2009.
- (7) (a) Jia, J.; Wu, H.-S.; Chen, Z.; Mo, Y. *Eur. J. Org. Chem.* **2013**, *2013*, 611–616. (b) Johansson, M. P.; Olsen, J. J. *Chem. Theory Comput.* **2008**, *4*, 1460–1471. (c) DeRider, M. L.; Wilkens, S. J.; Waddell, M. J.; Bretscher, L. E.; Weinhold, F.; Raines, R. T.; Markley, J. L. *J. Am. Chem. Soc.* **2002**, *124*, 2497–2505.
- (8) Tomasi, J.; Mennucci, B.; Cancès, E. *J. Mol. Struct.: THEOCHEM* **1999**, *464*, 211–26.
- (9) (a) Mitoraj, M. P.; Michalak, A.; Ziegler, T. *J. Chem. Theory Comput.* **2009**, *5*, 962–975. (b) Kurczab, R.; Mitoraj, M. P.; Michalak, A.; Ziegler, T. *J. Phys. Chem. A* **2010**, *114*, 8581–8590. (c) Dyduch, K.; Mitoraj, M. P.; Michalak, A. *J. Mol. Model.* **2013**, *19*, 2747–2758.
- (10) Pettersen, E. F.; Goddard, T. D.; Huang, C. C.; Couch, G. S.; Greenblatt, D. M.; Meng, E. C.; Ferrin, T. E. *J. Comput. Chem.* **2004**, *25*, 1605–1612.
- (11) Carey, F. A.; Sundberg, R. J. *Advanced Organic Chemistry, Part A: Structure and Mechanisms*, 5th ed.; Springer: New York, 2007; p 339.
- (12) In support of this assertion, the C=O bond length of *p*-nitrobenzaldehyde minimized at the B3LYP/6-31G(d) level of theory was calculated to be 1.214 Å, while that of (*p*-dimethylamino) benzaldehyde was calculated to be 1.220 Å.
- (13) te Velde, G.; Bickelhaupt, F. M.; Baerends, E. J.; Fonseca Guerra, C.; van Gisbergen, S. J. A.; Snijders, J. G.; Ziegler, T. *J. Comput. Chem.* **2001**, *22*, 931–967.